Micrometer-resolution 3D imaging Lidar based on metalens with strong chromatic dispersion

Wang Lu[a,b], Wang Xin[a,b,*]
[a] School of Optics and Photonics, Beijing Institute of Technology, Beijing 100081, China;[b]Beijing Key Laboratory for Precision Optoelectronic Measurement Instrument and Technology, Beijing 100081, China

*wangxin@bit.edu.cn

ABSTRACT

In recent years, metalens showed their applied potential as depth information sensors. To combine the advantages of active-imaging Lidar and the depth information acquisition ability of metalens, a 3D imaging setup based on metalens array with strong chromatic dispersion was proposed in this paper. When the scene was illuminated by the laser with different wavelengths, the point spread function (PSF) of points in the scene was varied at a certain imaging plane behind the metalens. Only when the point located on the object plane was illuminated by a certain wavelength the optimized PSF could be observed on the imaging plane. Therefore, by measuring the PSFs of a pairs of defocus images induced by the chromatic dispersion of the metalens the absolute distance from metalens to a point on the scene could be obtained. Combined with the clear 2D image, 3D imaging can be realized. When the chromatic dispersion of the metalens is stronger, PSF is more sensitive to the distance change, higher distance measurement resolution can be obtained. The simulation results of metalens with different dispersion shown in the paper proved our assumption.

Keywords: metalens, chromatic dispersion, 3D Lidar

1. INTRODUCTION

3D scene reconstruction has a widely applied in autonomous vehicles, artificial intelligence, life science and industrial product inspection. Ordinary optical imaging can only obtain two-dimensional information. To obtain depth information, the techniques such as time-of-flight (TOF)[1] based on pulsed laser, absolute range measurement using femtosecond laser, and coherence ranging based on optical interference principle are usually used. However, due to the limitation of the pulse width, the resolution of time-of-flight measurement is in the millimeter level. Although femtosecond laser ranging technique based on coherence measurement has the highest resolution[2,3], but the requirement of light source is strict and the cost is high. Moreover, the interferometry is very sensitive to perturbation along the optical paths.

Depth estimation based on defocus effect has been proposed in 1980s. But the measurement resolution and dynamic range are limited by the depth of focus of traditional imaging optics. Metalens is an artificially manufactured component that can control the amplitude, polarization, and phase of the incident light. Compared with traditional optical devices, the point spread function (PSF) can be flexibly engineered. In addition, metalens has small size and can be easily integrated with other photoelectric components. These advantages make metalens to be a superior imaging device for depth estimation. t. Many achievements have been made in this field. For example, Shane Colburn et al. designed a dual-aperture metasurface element with double-helix PSF (DH-PSF)[4]. It consisted of two spatially separated but adjacent metasurfaces. This monocular passive ranging scheme had a ranging error of 1.7%. Liu et al. used three hexagonal metalens to form an array[5]. Depth information was derived by the translation relationship of the three images from different hexagonal metalens. By designing a gradient descent algorithm to correct aberrations, a multi-eye visual ranging setup with accuracy in the micron level was demonstrated. The relative ranging error was 0.6% to 1.31%.

In this paper we proposed an active 3D imaging setup based on high dispersive metalens array. By tuning the wavelength of the illuminating laser, the images with different PSFs were captured on a fixed imaging plane. Benefiting from the high degree of differentiation of PSFs induced by strong dispersion of the metalens, the depth estimation error

SPIE-CLP Conference on Advanced Photonics 2022, edited by Xu Liu, Anatoly Zayats, Xiaocong Yuan, Proc. of SPIE Vol. 12601, 126010Q
 · 0277-786X · doi: 10.1117/12.2667156

of 5μm was realized. Combine the distance information with the 2D imaging of the metalens array. 3D imaging could be obtained. This method avoids the complicated metalens manufactory and the mechanical motion.

2. 3D IMAGING SETUP AND DEPTH ESIMATION PRINCIPLE

The schematics of the active 3D imaging setup is shown in Fig. 1.A wavelength tunable laser is used as the illumination source. The output beam of the laser was collimated. Then, a beam shaper is used to generate desired illumination for the measured object. With the illumination the object is imaged by the metalens array. A microscope objective is used to magnify the image, and a camera is used to capture the magnified image.

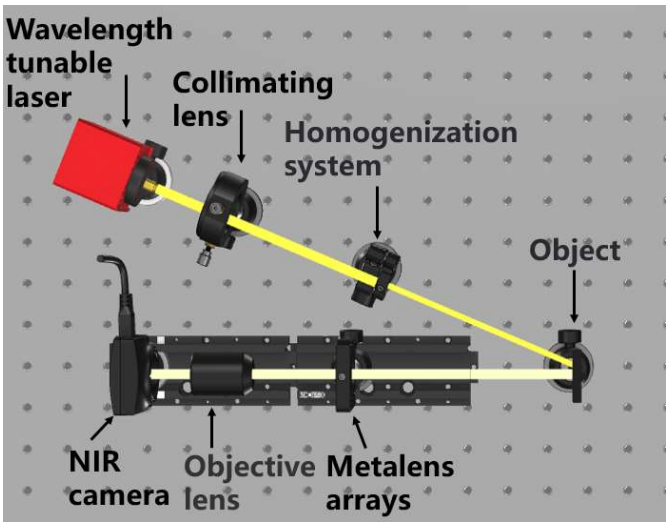

Figure 1. schematics of the active ranging setup

When the metalens has chromatic dispersion, the point source located at a certain distance from the metalens has different imaging distances for different working wavelengths[6]. For example, if the images of the object illuminated by three different wavelengths were captured, as indicated in Fig. 2 only one of them is on focus (green line) and the others are defocus (red and blue lines). With the known relationship between the PSFs and defocus distances at different wavelengths, the distance of the point source can be retrieved through the three PSFs.

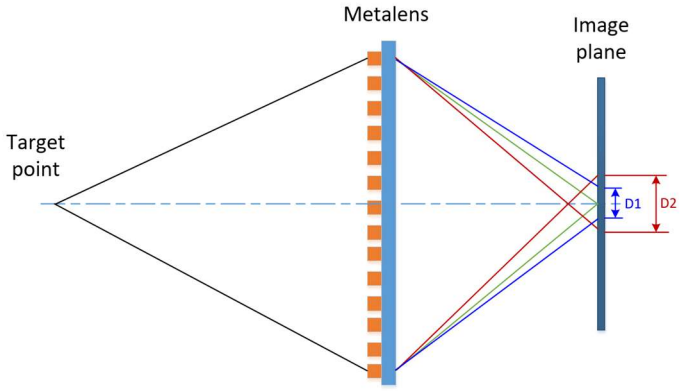

Figure 2. distance measurement principle based on metalens chromatic dispersion

When a metalens array was used, the points on the object surface will be imaged by individual metalens. Afterwards, the distances of these points could be derived. Combining the distance mapping with the clear on focus 2D imaging, 3D imaging of the object was reconstructed. The 3D imaging acquisition flow is shown in Fig. 3.

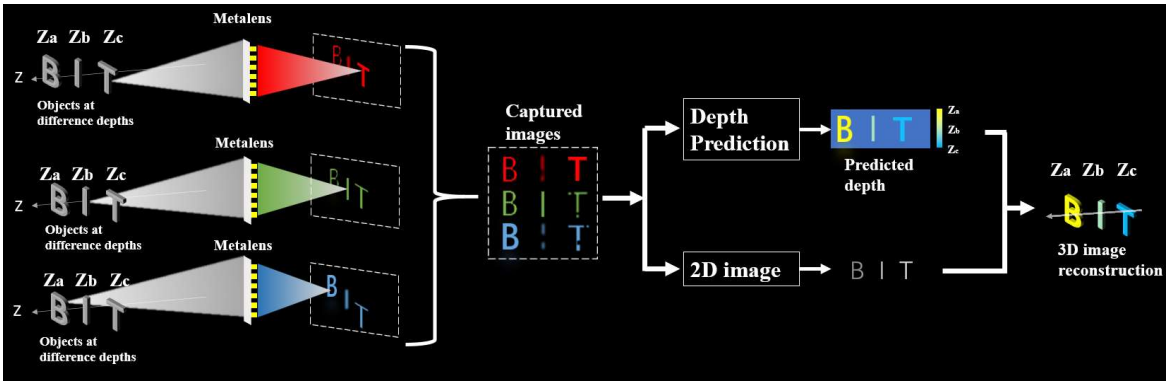

Figure 3. 3Dimaging acquisition flow

The distance of every point on the object surface can be calculated by[7]

$$Z(x,y) = (\alpha + \beta \frac{F*\delta I(x,y)}{F*\nabla^2 I(x,y)})^{-1} \quad (1)$$

with $\alpha = \frac{Z_{f-}+Z_{f+}}{2Z_{f+}Z_{f-}}$ and $\beta = -\frac{1}{(\Sigma Z_s)^2}\frac{Z_{f+}Z_{f-}}{Z_{f-}-Z_{f+}}$, where $Z_{f\pm}$ are the in-focus distance for two different wavelength illuminations, Z_s is the sensor distance, $\boldsymbol{\Sigma}$ is the entrance pupil size. The other parameters $\delta I = I_+(x,y) - I_-(x,y)$ and $\nabla^2 I(x,y) = \frac{1}{2}\nabla^2(I_+(x,y) - I_-(x,y))$ are the image intensity difference and the averaged spatial Laplacians at each pixel, respectively. The F in Eq.1 is a linear filter. $\nabla^2 I(x,y)$ can be estimated as $\frac{\delta I(x,y)}{\delta\sigma}$ via a finite difference. After calculation, we can simplify Eq.1 to

$$Z = \frac{\frac{\delta I(x,y)}{\delta\sigma}}{\alpha+\beta'\frac{I_+(x,y)-I_-(x,y)}{Z_{f-}-Z_{f+}}} \quad (2)$$

where α is the constant associated with $Z_{f\pm}$, $\beta' = -\frac{Z_{f+}Z_{f-}}{(\Sigma Z_s)^2}$ is the constant associated with Z_s , Σ and $Z_{f\pm}$. According to Eq.2, when metalens array with strong chromatic dispersion is used, large $Z_{f-} - Z_{f+}$will make Z more sensitive to the intensity distribution difference $(I_+(x,y) - I_-(x,y))$ that is, the ranging accuracy is improved, as shown in Fig. 4.

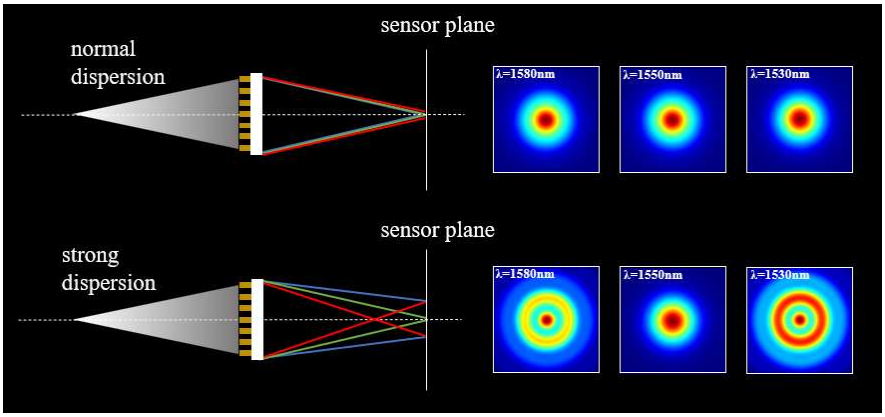

Figure 4. PSFs comparison of metalens with different chromatic dispersions

3. METALENS WITH STRONG CHROMATIC DISPERSION

The main function of the metalens is to image object. Generally speaking, there are two phase modulation techniques, named as geometric phase and propagation phase. The geometric phase, also known as Pancharatnam-Berry(PB) phase, is

formed by the design of single antenna with spatial rotation arrangement. It is independent of the incident wavelength but has requirements on the polarization state of the incident light. As comparison, the propagation phase is controlled by changing the geometric parameter of the single antenna. When symmetric unit shape is used, the phase shift is independent to the incident light polarization but is sensitive to the incident light wavelength. In order to obtain wavelength dependent phase changing, propagation phase is used in our design. The normal metalens phase profile for different wavelengths is given by[8]

$$\varphi(x,y) = \frac{2\pi}{\lambda}\left(f - \sqrt{x^2 + y^2 + f^2}\right) \tag{3}$$

where λ is the incident wavelength, x and y are the spatial coordinates on the metalens, and f is the designed focal length.

Rewriting Eq. 3 to

$$f = \frac{\varphi(x,y)}{4\pi} - \pi \cdot \frac{x^2+y^2}{\varphi(x,y)\lambda} \tag{4}$$

it shows that the focus length depends on the incident wavelength. When we choose a focus length f_0 and a center wavelength λ_0 to design a phase profile $\varphi_0(x,y)$, the focus length will decrease with the wavelength increasing.

Differentiating both sides of Eq. 4 by λ, we obtain

$$\frac{df}{d\lambda} = -\pi \cdot \frac{x^2+y^2}{\varphi(x,y)\lambda^2} \tag{5}$$

It means bigger focus length changing can be achieved by using longer wavelength. So, we choose the 1550 nm as center wavelength, which is infrared. Moreover, tunable laser covering the wavelength range of 1530 nm to 1610 nm is the commonly used laser source in fiber communication.

To obtain stronger chromatic dispersion a programmable phase $\varphi_{code}(\lambda)$ related to incident light wavelength is added,

$$\varphi(x,y) = \frac{2\pi}{\lambda}\left(f - \sqrt{x^2 + y^2 + f^2}\right) - \varphi_{code}(\lambda) \tag{6}$$

where $\varphi_{code}(\lambda)$ can be engineered by geometric design of the single antenna. Cuboid shown in Fig.5 (A) was used in our design. The radius of the metalens is 20 μm and the focal length is 220 μm. In this paper, silicon dioxide is used as the substrate and zinc oxide is used to form the cuboids. The geometric parameters of metalens surface structure are cell period(*P*), cuboid height(*H*) and cuboid side length(*L*). To obtain the phase profile required by metalens, the phase shift should cover 0 to 4.2 rad, which was obtained by varying the side length *L* with fixed period *P* and height *H*. In addition, the transmittance of the unit cells should be high and uniform. Here, the period *P* and height *H* were chosen to be 1.5 μm and 2.1 μm, respectively. The phase shifted from 0 to 4.2 rad when the side length *L* was scanned from 0.1 μm to 0.7 μm. The propagation phase shifts formed by the cuboids are shown in Fig. 5 (B) with the corresponding transmission. During the entire side length scanning range, the transmission of the antennas was higher than 0.88. It will benefit the high efficiency of the metalens.

Because the phase shift within the entire metalens radius was lower than 2π, these antennas only need to be arranged once. To facilitate manufacturing the period *P* was optimized. Therefore, 14 cuboids with different side lengths were used along metalens radius. The calculated phase profile of the metalens (marked by Target) is shown in Fig.5 (C) together with the phase profile formed by cuboids (marked by Simulation). They are coincide with each other. The fluctuation of the simulated phase profile was caused by the discrete phase distribution.

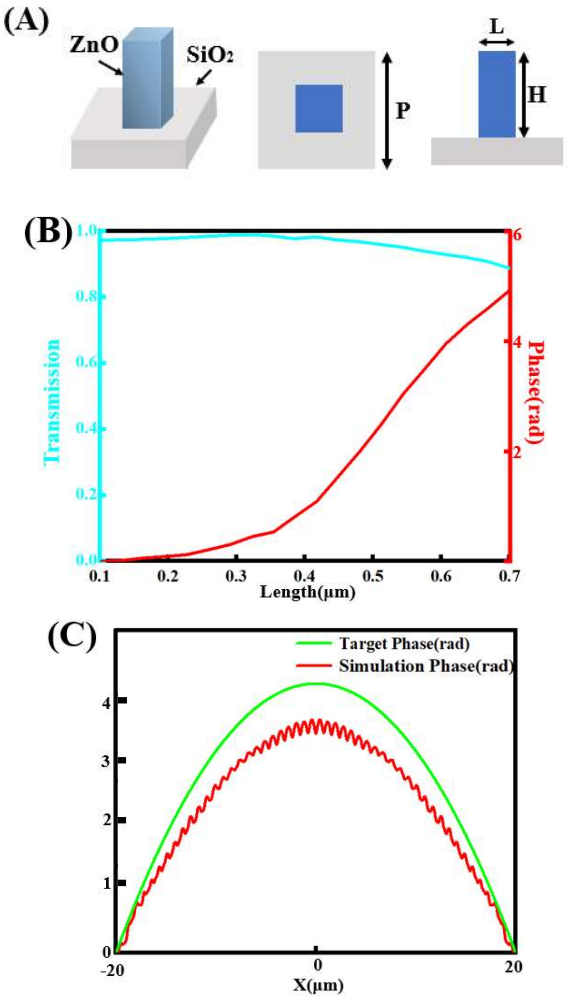

Figure 5. Metalens design. (A) structure of the metalens unit cell, (B) the phase shift and the transmission as a function of side length of ZnO cuboid, (C) calculated phase profile and the phase profile formed by cuboids.

We used finite-difference time-domain simulation software to simulate the performance of the metalens. With a plane incident wave at 1550 nm the focus point locates at 214 μm, as shown in Fig. 6, the PSF width is 15.1 μm. The focusing efficiency was about 34.9%.

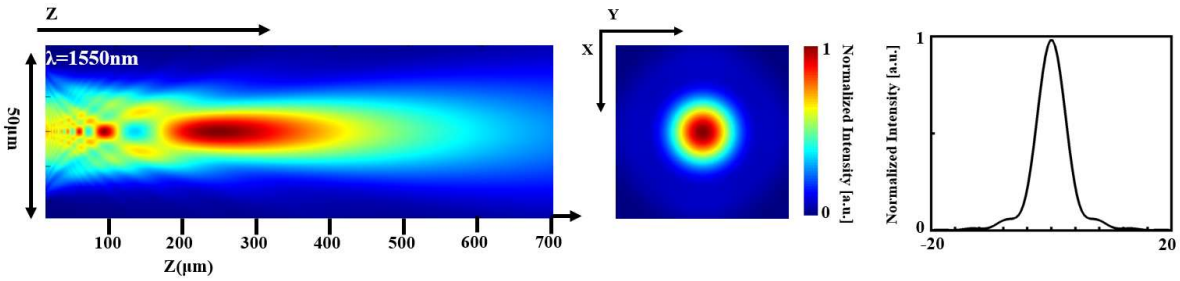

Figure 6. Focusing simulation of the metalens with incident plane wave at 1550 nm.

The chromatic dispersion of the metalens was compared with a metalens form by circular columns (shown in Fig.7 (A)). The simulated focusing results for the incident plane waves at 1530 nm, 1550nm and 1580 nm wavelengths are shown in Fig.7 (B) and (C). The focal length of the metalens formed by circular columns varies from 213 μm to 218 μm, while metalens formed by cuboids shows larger focal length changes, from 232 μm to 244 μm. With all these illumination

wavelengths, both metalens showed good focusing ability. The PSF width with 1550 nm illumination was taken as the reference, PSF width variation with wavelengths is shown in Fig. 7 (D). For cuboid-metalens, the PSF width varied by 0.76 μm, while for circular columns-metalens, the value was 0.46 μm. With the increase of the chromatic dispersion, the change of the PSF width was also larger, which will induce high distance estimation accuracy. Fig. 7 (E) shows the focal length changes of the both metalens when varying of the incident light wavelength. The bigger change slop and larger change range meant that the metalens formed by cuboids had stronger chromatic dispersion than that of metalens formed by circular columns[8].

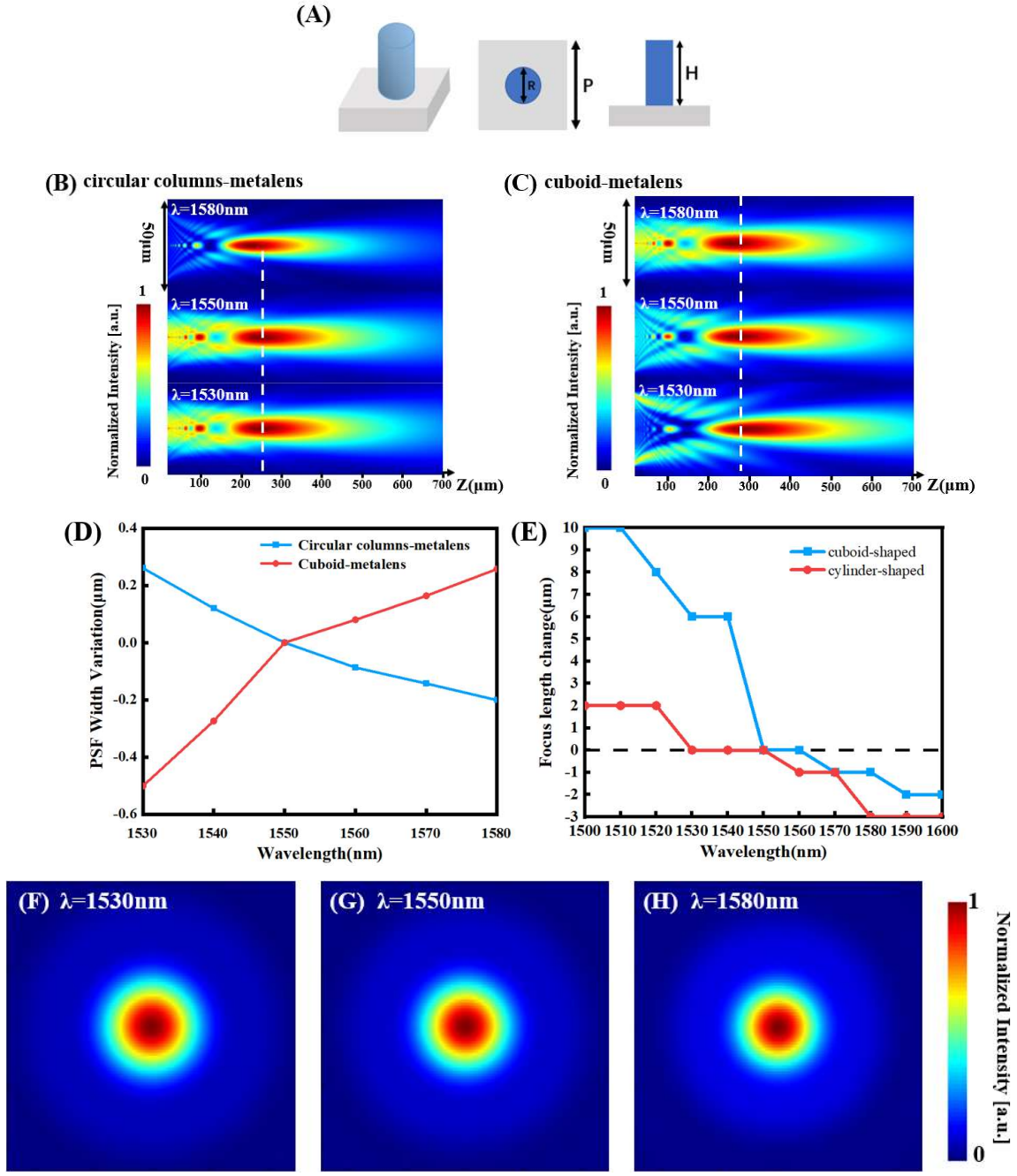

Figure.7 Focus length simulation. (A) unit cell structure of circular columns, (B) focusing of the incident plane waves with different wavelengths by metalens formed by cuboids, (C) focusing of the incident plane waves with different wavelengths by metalens formed

by circular columns, (D) PSF width variation with the incident light wavelength, (E) focal length changes as a function of incident light wavelengths. (F)(G)(H) focal plane spot at different wavelength incident.

4. DISTANCE ESTIMATION

To simply illustrate the distance estimation, a point source located 300 μm in front of the metalens was used as an example. For the center wavelength ($\lambda_0 = 1550\ nm$) illumination, the imaging plane was located at 1064 μm behind the metalens with focal length of 234 μm, according to the thin lens image principle. So, we set a sensor screen 1064 μm behind the metalens in simulations. The image of the point source is shown in Fig. 8 (A). The diameter of the imaging spot was 15 μm, which was equal to the PSF width.

When we changed the wavelength of the point source, the PSF variation were observed, as shown in Fig. 8 (B) and (C). With 1530 nm and 1580 nm the strong defocus phenomenon showed. Based on the distance estimation principle described in Section. 2, in this case, the clear 2D image was obtained by 1550 nm illumination; and the distance could be derived by either pair of PSFs were captured at three different wavelengths. Combining clear 2D image and the distance of the point source, 3D imaging can be constructed.

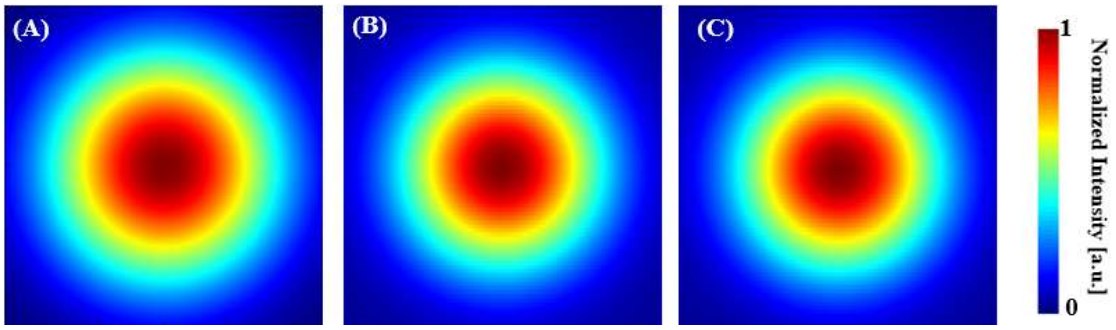

Figure 8. PSFs of (A) 1530 nm illumination, (B) 1550 nm illumination, (C) 1580 nm illumination

To further illustrate our 3D imaging method, the imaging of point sources located at 298 μm, 310 μm were simulated. The senser screen was still set at 1064 μm. The simulation results are shown in Fig. 9. The clear 2D images were observed at 1530 nm illumination and 1580 nm illumination, respectively. According to the simulation results in Fig. 7 (E) and the thin lens image principle, the retrieved point source distances were 295 μm, 305 μm and 315 μm. The corresponding distance estimation error was 3 μm, 5 μm and 5 μm.

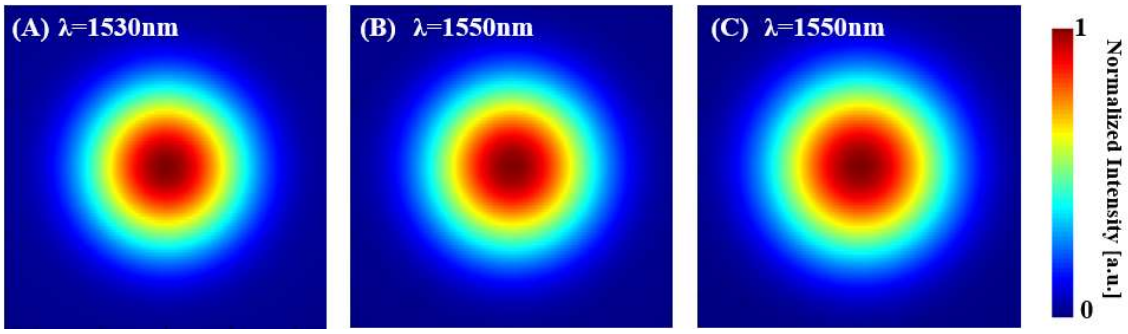

Figure 9 Simulation results of the point sources located at (A) 298 μm, (B) 300 μm and (C) 310 μm.

The same simulations were made using metalens formed by circular columns, the estimated point source distances were 305 μm, 310 μm and 320 μm, respectively. The corresponding distance estimation error were 7 μm, 10 μm and 10 μm. which is bigger than the above results. The simulation results meant that using the metalens with stronger chromatic dispersion the distance estimation error could be reduced.

5. CONCLUSION

This paper proposes an active 3D imaging method based on wavelength-dependent PSF variation of a metalens. The designed lens consists of an array of periodic zinc oxide cuboids placed on silicon dioxide substrate. Considering the difficulty of the subsequent manufacturing, the period of the metalens unit optimized. We simulated the focusing effect of the designed metalens with different incident wavelengths and clear and symmetrical focusing spots were observed. Based on the metalens distance estimation experiments were made. When the point source was set at 298 μm, 300 μm and 310 μm, the estimated distances were 295 μm, 305 μm and 315 μm. The minimum error is 3 μm. The experimental results proved the proposed 3D imaging method. In addition, by comparison with a commonly used metalens formed by circular columns, the metalens with stronger chromatic dispersion showed lower distance estimation error. We believe when a 3D object is imaged by the metalens array, the clear 2D image can be obtained through illumination wavelength scan, and the distance mapping can be derived by defocus PSF and distance relation. These 3D imaging methods show great potential applications in biomedicine, material science and product inspection.

REFERENCES

[1] Oggier T, Lehmann M, Kaufmann R, et al. An all-solid-state optical range camera for 3D real-time imaging with sub-centimeter depth resolution (SwissRanger) Optical Design and Engineering. International Society for Optics and Photonics, 2004, 5249: 534-545.

[2] Lee J, Kim Y J, Lee K, et al. Time-of-flight measurement with femtosecond light pulses. Nature Photonics,2010,4(10):207-207.

[3] Liu T A,Newbury N R,Coddington I.Sub-micron absolute distance measurements in sub-millisecond times with dual free-running femtosecond Er fiber-lasers. Optics Express,2011,19(19):18501-9.

[4] Colburn, S and Majumdar, A. Metasurface Generation of Paired Accelerating and Rotating Optical Beams for Passive Ranging and Scene Reconstruction. Jun 17 2020 | ACS PHOTONICS 7 (6) , pp.1529-1536

[5] Liu W W, Ma D N, Li Z C, et al. Aberration-corrected three-dimensional positioning with a single-shot metalens array. Optica 2020,7(12):1706-1713.

[6] Shiyu Tan, Frank Yang, Vivek Boominathan, Ashok Veeraraghavan, and Gururaj V. Naik. 3D Imaging Using Extreme Dispersion in Optical Metasurfaces. ACS Photonics 2021,8 (5):1421-1429.

[7] Guo, Q. et al. Compact single-shot metalens depth sensors inspired by eyes of jumping spiders. Proc. Natl Acad. Sci. USA 116, 22959–22965 (2019).

[8] M. Khorasaninejad, W. T. Chen, A. Y. Zhu, et al. Multispectral chiral imaging with a metalens. Nano Lett., vol. 16, no. 7, pp. 4595–4600, 2016.